Per. Mineral. (2008), 77, 63-77

doi:10.2451/2008PM0005
http://go.to/permin

PERIODICO di MINERALOGIA
established in 1930

An International Journal of
MINERALOGY, CRYSTALLOGRAPHY, GEOCHEMISTRY, ORE DEPOSITS, PETROLOGY, VOLCANOLOGY
and applied topics on *Environment*, *Archaeometry* and *Cultural Heritage*

Intra-crystalline relationships in the constituent phases of a spinel lherzolite xenolith from Predazzo (eastern Alps, northern Italy) and petrological implications

Anna Carraro *

Dipartimento di Geoscienze, Università degli Studi di Padova, Via Giotto, 1, 35137 Padova, Italy

Submitted, March 2007 - Accepted, December 2007

Abstract. — Upper mantle minerals of a spinel lherzolite xenolith from a Triassic mafic alkaline dyke of Predazzo (Dolomites, Eastern Alps) were investigated by combined single-crystal X-ray diffraction (SREF) and electron microprobe analyses (EMPA). Crystal chemical results indicated that clinopyroxene, orthopyroxene, olivine and spinel crystals are the most refractory products of a partial melting event, at the end of which constituent minerals assembled in protogranular texture in upper mantle equilibration conditions. Results also showed that cation distribution is extremely sensitive, especially when mantle mineral compositions are considered, and that intracrystalline thermometric calibrations should be used with caution. The intracrystalline closure temperatures calculated for clinopyroxenes (T = 589±80 °C), orthopyroxenes (T = 684±64 °C) and spinel (T = 782±31 °C), suggest a relatively fast cooling rate, consistent with the subvolcanic geological context in which the host dyke cooled. The mean equilibration pressure calculated from three olivine-clinopyroxene single-crystal pairs (P about 1.5 GPa) confirm data obtained on large non-isolated olivine-clinopyroxene pairs, and indicate that the lower equilibration pressures obtained for some olivine crystal rims cannot be the result of secondary fluorescence effects, but are only due to decompression and/or heating of the xenoliths and re-equilibration in shallower conditions, within the upper mantle or the lower crust.

* E-mail: a.carraro@unipd.it

Riassunto. — I minerali costituenti uno xenolite di lherzolite a spinello, contenuto in un filone femico alcalino dell'area di Predazzo (Dolomiti, Alpi Orientali), sono stati studiati mediante diffrattometria a cristallo singolo (SREF) e microanalisi (EMPA). I dati cristallochimici indicano che la paragenesi studiata (clinopirosseno, ortopirosseno, olivina e spinello) rappresenta il prodotto più refrattario di un evento di fusione parziale, al termine del quale i minerali si sono riequilibrati, con microstruttura protogranulare, alle condizioni di temperatura e pressione presenti nel mantello superiore. I risultati suggeriscono inoltre che la ripartizione cationica nei siti cristallini delle quattro fasi è estremamente sensibile, qualora si considerino composizioni naturali (minerali di mantello). Di conseguenza, anche i "geotermometri" intracristallini dovrebbero essere utilizzati con cautela. Le temperature di chiusura intracristallina stimate per il clinopirosseno (T = 589±80 °C), l'ortopirosseno (T = 684±64 °C) e lo spinello (T = 782±31 °C) indicano una velocità di raffreddamento relativamente veloce, coerente con il contesto subvulcanico in cui si è raffreddato il filone ospite. La pressione di equilibrio dello xenolite è stata stimata per tre coppie di cristalli

singoli di clinopirosseno e olivina. Il valore medio di 1,5 GPa conferma i dati ottenuti per coppie di grossi granuli non isolati: le più basse pressioni ottenute in alcuni casi alle periferie dei cristalli non sono causate dall'effetto della fluorescenza secondaria ma sono piuttosto dovute a decompressione e/o riscaldamento subiti dallo xenolite a profondità inferiori, nel mantello o nella bassa crosta, durante la risalita del magma ospite.

Key Words: *spinel lherzolite xenolith, intra-crystalline relationships, equilibration pressure, Predazzo, NE Italy.*

Introduction and petrological notes

Many studies in the last twenty-five years have demonstrated that crystal chemistry of minerals from upper mantle xenoliths (*i.e.*, clinopyroxene, orthopyroxene, olivine and spinel), obtained by SREF (X-Ray Single-Crystal Structure-Refinement), provides an essential contribution in studying the petrogenesis of alkaline mafic host rocks. Cation distribution in the structural sites of these mineral phases is related to crystallographic controls, which in turn depend on the petrological evolution of the host rock (Cundari *et al*., 1986). Site configurations of upper mantle phases are therefore the response to 1) melting and/or crystallisation processes within the upper mantle, and 2) cooling rate after transport of the xenoliths by host magma towards shallower conditions (Dal Negro *et al*., 1984). Moreover, the cooling history of the host rock can only be evaluated if accurate values of intra-crystalline temperature are obtained for each coexisting phase of mantle xenoliths, since these temperatures are related to the accuracy of data calculated for site occupancies (Princivalle *et al*., 1994).

The present work describes the intra-crystalline relationships which govern the cation ordering in the structural sites of all coexisting mantle minerals of a spinel lherzolite xenolith from the Triassic Magmatic Complex of Predazzo (NE Italy). The studied xenolith, labelled P91 7 C2, belongs to a group of upper mantle xenoliths contained in Triassic camptonitic dykes (234 Ma), which cooled in subvolcanic conditions. These xenoliths were described in details in Carraro and Visonà (2003) in terms of petrography, mineral chemistry and geothermobarometry. Xenolith P91 7 C2, hereafter named simply C2, is one of the protogranular textured xenoliths resulting from partial melting of the upper mantle, modified by partial re-crystallisation under decreasing temperature, in a regime of weak plastic deformation. It consists of forsteritic olivine (ol; $Fo_{91.0\text{-}92.6}$), enstatitic orthopyroxene (opx; $En_{88.6\text{-}92.0}Fs_{6.9\text{-}7.0}Wo_{1.1\text{-}4.5}$), diopsidic clinopyroxene (cpx; $Wo_{47.4\text{-}47.6}En_{48.7\text{-}49.7}Fs_{2.8\text{-}3.6}$) and Cr-bearing spinel (sp; Cr_2O_3 = 34.8-36.0 wt%), in order of decreasing abundance (Carraro and Visonà, 2003).

Additional important information about residua from partial melting events, which involved the upper mantle portion under the Dolomites, may also be obtained from site configurations of mantle minerals, in terms of crystal chemistry. Xenolith C2 is the only one from the Predazzo Area for which a detailed crystal chemical study on all four phases of the lherzolitic paragenesis was possible, as most of the olivine and orthopyroxene grains from other xenoliths were altered and/or not suitable for single-crystal X-ray data collection. Some cpx and opx crystals were previously studied by SREF (Carraro and Salviulo, 1998): those crystals labelled cpx B1 and B3, and opx B4, B5 and B6 correspond to cpx C2B1 and C2B3, and opx C2B4, C2B5 and C2B6, respectively, in the present paper. Crystal structure refinements were obtained using the STRUCSY program (copyright STOE, Germany). In this work, the same crystals were re-refined using SHELXL-93 program. As demonstrated by various studies from the literature (*e.g.*, Stimpfl *et al*., 1999; Domeneghetti *et al*., 2000), the experimental information is more fully exploited using SHELXL-93 refinement. This structure refinement strategy was also applied to all the investigated crystals.

Data of coexisting spinel crystals CRSP1, CRSP3 and CRSP4 were reported in Carraro (2003). They belong to a series of Cr-bearing spinels from the Predazzo Area, which are interpreted as representing successive steps of partial melting. Olivine data are reported here for the first time.

Crystal chemical features of four phases were compared with those of analogue minerals forming mantle xenoliths from the worldwide literature. In particular, the comparison was made using crystal chemical data obtained for the whole paragenesis of spinel peridotite xenoliths: such

complete data are reported for samples from 1) Mt. Leura, Mt. Porndon and Mt. Noorat, Victoria, Australia (Cundari *et al*., 1986; Dal Negro *et al*., 1984; Molin and Stimpfl, 1994; Princivalle *et al*., 1989a), 2) Cameroon (Princivalle *et al*., 1995; Princivalle *et al*., 2000a) and 3) Hannouba Region, China (Princivalle *et al*., 1998). Data from cation distribution were used to estimate intra-crystalline closure temperatures with appropriate thermometric calibrations. Lastly, estimation of equilibration pressure was made by applying the Ca-in-ol geobarometer of Köhler and Brey (1990) to the composition of olivine and clinopyroxene single-crystal pairs.

Fig. 1 shows the compositional relationships among mantle xenolith assemblages, in terms of Cr# (=Cr/(Cr+Al)) ratio of spinel *vs*. cpx modal content, Mg# (= Mg/(Mg+Fe^{2+})) of cpx and opx, and Fo content in olivine. The comparison also takes into account compositions of opx and ol (NE Brazil: Princivalle *et al*., 1989b; Princivalle *et al*., 1994; Princivalle *et al*., 1999; Nemby, Paraguay: Princivalle *et al*., 2000b) for which crystallographic and cation distribution data are not available from literature. It may be observed that the Predazzo mantle xenolith has cpx modal content (6.3 Vol. %) similar to that of samples from NE Brazil (PR series), Mt. Noorat and Paraguay, but differs from the Mt. Leura samples, for which cpx modal contents are higher. However, xenolith C2 has cpx modal proportion consistent with the trend followed by upper mantle samples, which experienced pure fractional melting and resulted in protogranular texture (Hellebrand *et al*., 2001). Moreover, the studied crystals have compositions similar to those of the other compared samples, except for the Mt. Noorat samples, which have lower Mg# of cpx.

Experimental

Crystals from the Predazzo mantle xenolith were carefully selected under a petrographic microscope and hand-picked from a section *ca*. 100 µm thick. Only unaltered, optically homogeneous crystal fragments were chosen for single-crystal data collection; selected pyroxene grains were free from exsolution lamellae. Crystals were 0.06 to 0.12 mm in their largest

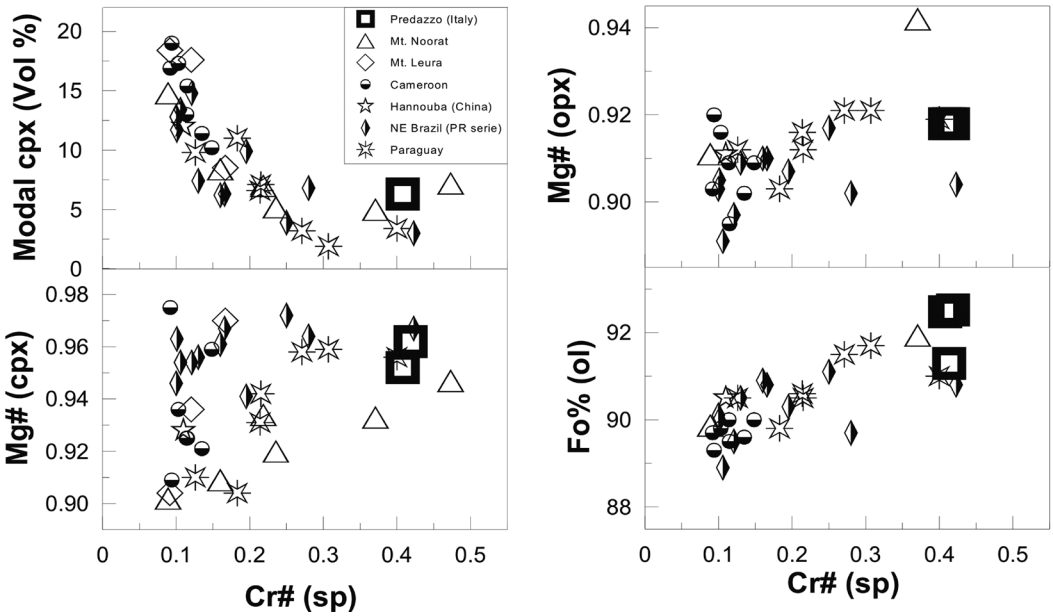

Fig. 1 – Cr# (= Cr/(Cr+Al)) of spinel *vs*. cpx modal content, Mg# (= Mg/(Mg+Fe^{2+})) of cpx and opx, and Fo content of olivine for xenolith C2 from Predazzo. Samples from literature are reported for comparison (see text for references).

dimension. X-ray diffraction data were recorded by means of an automated single-crystal STOE AED4 four-circle diffractometer using MoK_α (λ = 0.7107 Å) radiation monochromatised by a flat graphite crystal. Experimental conditions for X-ray data collection are listed in Table 1. Structural refinements, performed with the SHELXL-93 program (Sheldrick, 1993), gave the best disagreement factors using scattering curves (International Tables for X-ray Crystallography, 1974; Tokonami, 1965) in the following way: fully ionised Mg^{2+} *vs*. Fe^{2+} and Ca^{2+} *vs*. Na^{+} in clinopyroxene M1 and M2 sites, respectively; fully ionised Mg^{2+} *vs*. Fe^{2+} in both M1 and M2 sites of orthopyroxene and olivine; completely neutral Mg *vs*. Fe and Al *vs*. Cr in spinel T and M sites, respectively. Partially ionised curves for Si and oxygen ($Si^{2.5+}$ and $O^{1.5-}$) were adopted for clinopyroxene, orthopyroxene and olivine, and partial ionisation for oxygen ($O^{0.9-}$) was used in spinel. For clinopyroxene, final Fourier difference syntheses did not reveal significant residual density (*i.e.*, M2' site; Rossi *et al*., 1987).

The same crystals used for X-ray single-crystal data collection were analysed for chemical composition with a Cameca/Camebax electron microprobe operating at 15 kV and 15 nA sample current. A PAP-CAMECA program was used to convert X-ray counts into oxide weight percentages (details in Carraro, 2003). Fifteen point analyses were performed on each olivine crystal: samples showed good chemical homogeneity, except for Ca. Accurate measurements of this element were carried out on a CAMECA SX50 microprobe operating at 20 kV and 55 nA, with an integration time of 300 s, using a special CAMECA analysis program for trace elements. Ca-rich clinopyroxene was used as a standard for calibration. The accuracy of analyses was checked with the SC/SN8323 olivine standard (Fuchs and Badia, pers. comm.) which contains 590 ± 5 ppm Ca. The microprobe analysis reproduced this value within ± 30 ppm.

Cation distributions between crystallographic sites of clinopyroxene, orthopyroxene, olivine and spinel were calculated by a minimisation program, taking into account structural and chemical data and following the procedures reported in Dal Negro *et al*. (1982) for clinopyroxene and orthopyroxene, Della Giusta *et al*. (1990) for olivine, and Lavina *et al*. (2002) for spinels. Structural data,

Table 1 – *Experimental conditions for X-ray data collection used for studied olivine, clinopyroxene, orthopyroxene and spinel*

	CPX	OPX	OL	SP
Space group	C 2/c	P b c a	P b n m	F d 3 m
Current and voltage	25mA, 45 kV	25mA, 45 kV	25mA, 45 kV	30mA, 55kV
2θ range	3-70°	3-70°	3-70°	3-110°
$Time_{min\text{-}max}$ per step	0.5–1.0 (1.5) s.	0.5–1.0 (1.5) s.	0.5 – 1.5 s.	0.6 – 1.2 s.
HKL min.	-15, -13, 0	-26, 0, 0	-7, 0, -9	0, 0, 0
HKL max.	15, 13, 8	26, 12, 7	7, 16, 9	19, 19, 19
Common conditions for all crystals:				
I/sigma		3-20		
Scan width		2.0°		
Scan method		ω/2θ (= 1.0)		
Temperature		296 K		
Corrections		Lorentz, polarization		
Absorption correction		North *et al*., (1968)		

mean chemical data and site partitioning of the investigated minerals are listed in Tables 2 and 3, respectively.

Crystal chemistry

Clinopyroxene

The studied crystals are characterised by high Ca and Mg contents (Ca = 0.83 a.f.u. and Mg = 0.85-0.86 a.f.u., respectively), plot within the diopside field in the conventional pyroxene quadrilateral and may be classified as chromian diopside (Cr = 0.05 a.f.u.; Morimoto *et al.*, 1988). Figs. 2a, 2c and 2e show cell volume (V_{cell}) *vs*. site volume variations, together with the data of analogue mantle cpx from the literature (see legend). The general positive trends shown by well known samples (Fig. 2c and 2e) are also followed by the Predazzo cpx. Moreover, their cell and site volumes (V_{cell}, VT, VM2 and VM1, respectively) are quite similar to those of Mt. Noorat (Victoria) but different from those of Cameroon, Mt. Leura, Mt. Porndon and Hannouba. Analogies in structural site volumes between Predazzo and Mt. Noorat cpx generally reflect similar crystal chemistry (*e.g.*, ^{IV}Al content in T site), except for (Ca+Na) content, which is higher for the Predazzo samples. On the other hand, differences in cell and volume sites between Predazzo and Mt. Leura cpx do not appear to be closely related to different cation distribution. For example, for similar ^{IV}Al contents, the VT of Predazzo cpx is higher than that of Mt Leura cpx (Fig. 2b). In Fig. 2f, the Predazzo cpx conform quite well to the linear increase in VM1, which is controlled by the decrease in R^{3+}. The studied samples also have VM1 and R^{3+} very similar to those of some crystals from the Victoria Region (Mts. Leura, Noorat and Porndon series), but with a slightly higher V_{cell} (Figs. 2e and 2f).

Orthopyroxene

The Predazzo opx crystals have high Mg and Fe contents (Mg = 1.73-1.74 a.f.u; Fe_{tot} = 0.15-0.16 a.f.u., respectively) and plot within the enstatite field in the conventional pyroxene quadrilateral (Morimoto *et al*., 1988). They have Mg# of 0.918 and Al content in the octahedral

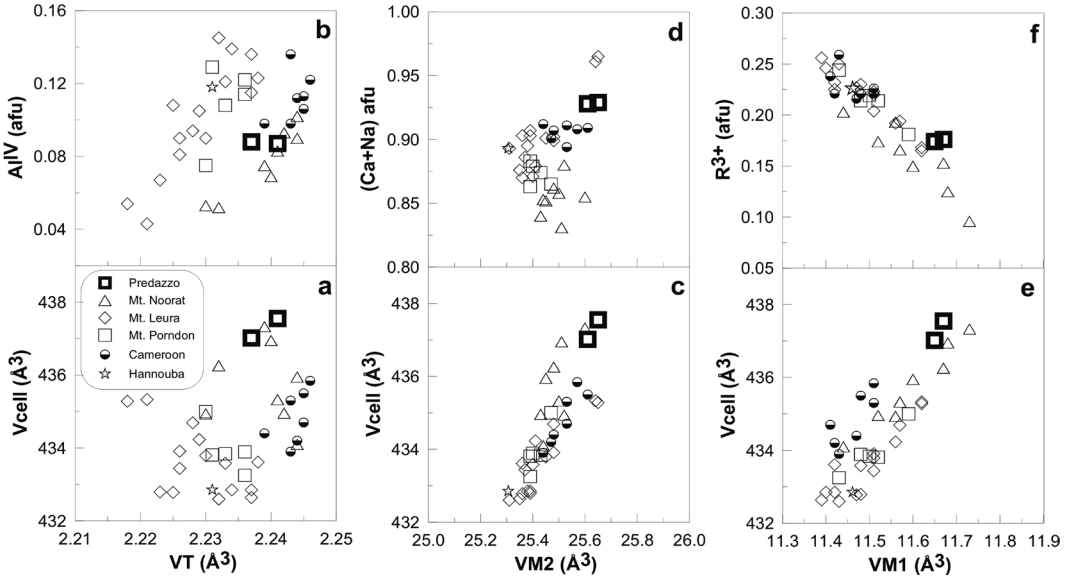

Fig. 2 – VT *vs*. V_{cell} (a) and *vs*. Al^{IV} (b), VM2 *vs*. V_{cell} (c) and *vs*. (Ca+Na) (d), VM1 *vs*. V_{cell} (e) and *vs*. R^{3+} content (f) for Predazzo cpx. Mantle xenolith cpx from Mts. Leura, Noorat and Porndon, Australia (Cundari *et al*., 1986; Dal Negro *et al*., 1984), Cameroon (Princivalle *et al*., 1995; Princivalle *et al*., 2000a) and Hannouba Region (China; Princivalle *et al*., 1998) are reported for comparison.

Table 2 – *Structural data of cpx, opx, ol and spinel from Predazzo mantle xenolith. Other crystallographic and refinement data for spinel are reported in* Carraro *(2003)*

CPX	**C2B1**	**C2B3**	*OPX*	**C2B4**	**C2B5**	**C2B6**
a (Å)	9.727(2)	9.724(1)	***a (Å)***	18.263(6)	18.256(2)	18.260(4)
b (Å)	8.891(2)	8.888(2)	***b (Å)***	8.829(2)	8.824(1)	8.825(2)
c (Å)	5.269(1)	5.266(1)	***c (Å)***	5.197(2)	5.197(1)	5.195(1)
β	106.23(2)	106.22(1)	**Vcell (Å³)**	838.07	837.33	837.16
Vcell (Å³)	437.55	437.02	**No. Obs. Rifl.**	2594	1218	1222
No. Obs. Rifl.	965	964	***R4σ***	0.043	0.02	0.029
R4σ	0.022	0.021	***wR2***	7.05	4.86	4.86
wR2	4.31	3.97	**Goof**	0.632	0.968	0.86
Goof	0.885	0.873	**<M1-O>**	2.077(6)	2.075(3)	2.076(5)
<M1-O>	2.066(2)	2.065(2)	**VM1**	11.82(1)	11.77(1)	11.79(1)
VM1	11.67(1)	11.65(1)	**m.a.n. (M1)**	12.46(9)	12.53(6)	12.47(8)
m.a.n. (M1)	13.29(8)	13.44(8)	**<M2-O>**	2.166(6)	2.163(3)	2.164(5)
<M2-O>	2.495(3)	2.494(3)	**VM2**	12.66(1)	12.61(1)	12.63(1)
VM2	25.65(1)	25.61(1)	**m.a.n. (M2)**	14.35(8)	14.15(6)	14.26(8)
m.a.n. (M2)	19.0(1)	18.8(1)	**<TA-O>**	1.627(4)	1.629(2)	1.627(4)
<T-O>	1.639(2)	1.638(2)	**TA-Obrg**	1.655	1.655	1.654
T-Obrg	1.675	1.673	**TA-Onon brg**	1.599	1.603	1.600
T-Onon brg	1.603	1.603	**VTA**	2.182(1)	2.189(2)	2.181(2)
VT	2.241(1)	2.237(1)	**<TB-O>**	1.645(5)	1.647(2)	1.646(4)
			TB-Obrg	1.679	1.68	1.679
			TB-Onon brg	1.612	1.614	1.614
			VTB	2.270(3)	2.275(2)	2.274(2)

M1 site close to 0.04 afu (see Tab. 3). In general, cation substitution Al^{VI}↔Mg mainly controls the configuration of M1 site in the opx structure; this requires cation substitution Al^{IV}↔Si in the TB site, in order to satisfy the charge balance, as shown by trends in Figs. 3a, 3b and 3c. We observe that the Al^{VI} content of Predazzo opx is lower than that of Cameroon (Al^{VI} = 0.066 afu) and Hannouba (Al^{VI} = 0.082 afu) opx, and intermediate with respect to that of the Australian opx series. The lower Al^{VI} content of the Predazzo crystals is consistent with a higher cell volume (837.16-838.08 Å³) with respect to those of Cameroon (V_{cell} = 835.99 Å³) and

TABLE 2 – *continued ...*

OL	**C2OL1**	**C2OL2**	**C2OL4**	**SP**	**CRSP1**	**CRSP3**	**CRSP4**
a (Å)	4.763(1)	4.763(1)	4.762(1)	***a (Å)***	8.214(2)	8.2139(8)	8.2129(9)
b (Å)	10.226(1)	10.225(1)	10.225(1)	***u***	0.2628(1)	0.2627(1)	0.2628(1)
c (Å)	5.995(1)	5.994(1)	5.993(1)	**No. Obs. Rifl.**	169	166	175
Vcell (Å³)	291.99(7)	291.92(5)	291.82(4)	***R4σ***	0.015	0.016	0.013
No. Obs. Rifl.	464	464	464	***wR2***	0.021	0.029	0.026
R4σ	0.028	0.015	0.016	**GooF**	0.856	0.872	0.953
wR2	6.88	2.97	3.00	**<T−O>**	1.961(1)	1.959(1)	1.960(1)
Goof	1.018	0.883	0.939	**m.a.n. (T)**	15.73(4)	15.69(6)	15.74(5)
<M1-O>	2.101(3)	2.102(2)	2.102(2)	**<M−O>**	1.954(1)	1.955(1)	1.954(1)
VM1	11.87(1)	11.89(1)	11.88(1)	**m.a.n. (M)**	17.21(4)	17.38(5)	17.24(3)
m.a.n. (M1)	13.4(2)	13.39(9)	13.31(9)				
<M2-O>	2.138(4)	2.136(3)	2.136(3)				
VM2	12.53(1)	12.50(1)	12.50(1)				
m.a.n. (M2)	13.2(2)	13.27(9)	13.23(9)				
<T-O>	1.634(4)	1.636(2)	1.635(2)				
VT	2.204(3)	2.210(2)	2.208(2)				

R4σ: residual index for reflections with I>4σ(I); wR2: weighted residual index for reflections with I>4σ(I); GooF: goodness of fit; m.a.n.: mean atomic numbers in considered sites. Numbers in brackets refer to standard deviation.

Hannouba (V_{cell} = 833.26 Å^3). Fe^{2+} is essentially ordered in M2 site (Fe^{2+}_{M1} = 0.01-0.02 afu), as in all compared samples.

Olivine

The Predazzo olivines have Fo content between 91.3 and 92.5%, which is only slightly higher than that reported for all compared samples. Fe^{2+} is slightly ordered in M1 site (Tab. 3), the volume of which is very similar to that of olivines from Mt. Leura, Cameroon and Hannouba, but lower than that of Mt. Noorat olivines, which contain a greater amount of Fe^{2+} in M1 (Fig. 4a). Similarly, cell volume values overlap some crystals from Mt. Leura (*e.g.*, LE9 and LE11; Princivalle and Secco, 1985) but are lower than those of Mt. Noorat samples (Fig. 4b).

Spinel

As previously stated, the Predazzo spinel crystals considered here were recently described in Carraro (2003), within a spinel series with variable Cr content. Due to the high Cr content of samples CRSP1, CRSP3 and CRSP4 (Cr = 0.783-0.811 afu), Mg^{2+} and Fe^{2+} are preferentially ordered in the tetrahedral T site (Tab. 3). Oxygen coordinate

Table 3 – *Mean chemical composition and site partitioning of cpx, opx, ol from studied mantle xenolith. Spinel data are from* Carraro *(2003)*

CPX	C2B1	C2B3
SiO_2	52.9(4)	53.1(2)
TiO_2	0.40(3)	0.38(4)
Al_2O_3	4.19(9)	4.03(7)
FeO	1.4(1)	1.1(1)
Fe_2O_3	0.81	1.23
MnO	0.09(4)	0.06(2)
MgO	15.7(2)	16.0(1)
CaO	21.4(3)	21.5(1)
Na_2O	1.43(8)	1.39(8)
Cr_2O_3	1.83(8)	1.71(9)
Sum	100.15	100.50
T SITE		
Si	1.913	1.912
Al^{IV}	0.087	0.088
Sum	2.000	2.000
M1 SITE		
Mg	0.812	0.81
Fe^{2+}	0.011	0.014
Fe^{3+}	0.021	0.033
Al^{VI}	0.092	0.083
Ti	0.011	0.010
Cr	0.052	0.049
Mn	0.001	0.001
Sum	1.000	1.000
M2 SITE		
Ca	0.828	0.831
Na	0.101	0.097
Mg	0.038	0.051
Fe^{2+}	0.031	0.02
Mn	0.002	0.001
Sum	1.000	1.000
$F(X_i)$ (1)	0.023	0.004
Ca+Na	0.929	0.928
$Mg\#$ (2)	0.952	0.962
R^{3+} (3)	0.176	0.175
k_D (4)	0.016	0.046
T (°C)	508.6	669.1

OPX	C2B4	C2B5	C2B6
SiO_2	56.1(3)	56.5(4)	56.4(3)
TiO_2	0.11(2)	0.12(3)	0.12(2)
Al_2O_3	2.63(8)	2.56(6)	2.55(2)
FeO	5.1(2)	5.4(1)	5.1(2)
Fe_2O_3	0.23	0.04	0.45
MnO	0.09(3)	0.14(6)	0.13(4)
MgO	33.7(7)	34.1(3)	34.3(1)
CaO	1.2(9)	0.6(1)	0.66(3)
Na_2O	0.06(5)	0.06(2)	0.07(3)
Cr_2O_3	0.7(1)	0.63(7)	0.69(5)
Sum	99.92	100.15	100.47
T SITE			
Si	1.873	1.878	1.876
Al^{IV}	0.127	0.122	0.124
Sum	2.000	2.000	2.000
M1 SITE			
Mg	0.923	0.919	0.924
Fe^{2+}	0.013	0.018	0.013
Fe^{3+}	0.000	0.000	0.000
Al^{VI}	0.043	0.042	0.041
Ti	0.003	0.003	0.003
Cr	0.018	0.017	0.019
Mn	0.000	0.001	0.000
Sum	1.000	1.000	1.000
M2 SITE			
Ca	0.047	0.024	0.024
Na	0.004	0.004	0.004
Mg	0.807	0.83	0.825
Fe^{2+}	0.140	0.138	0.144
Mn	0.002	0.004	0.003
Sum	1.000	1.000	1.000
$F(X_i)$ (1)	0.128	0.288	0.209
Ca+Na	0.051	0.028	0.028
R^{3+} (3)	0.064	0.062	0.063
k_D (4)	0.079	0.119	0.082
T (°C)	634.7	774	644

TABLE 3 – *continued ....*

OL	C2OL1	C2OL2	C2OL4
SiO_2	40.7(2)	40.8(3)	41.3(2)
FeO	8.1(2)	8.2(2)	8.5(2)
MnO	0.12(4)	0.13(4)	0.13(4)
MgO	50.5(4)	50.8(4)	51.0(2)
CaO	0.06(1)	0.06(1)	0.05(2)
NiO	0.38(5)	0.40(5)	0.00
Sum	99.86	100.39	100.98
T SITE			
Si	1.000	1.000	1.000
M1 SITE			
Mg	0.907	0.904	0.908
Fe^{2+}	0.086	0.088	0.092
Mn	0.000	0.000	0.000
Ni	0.007	0.008	0.000
Sum	1.000	1.000	1.000
M2 SITE			
Mg	0.919	0.917	0.920
Fe^{2+}	0.077	0.078	0.076
Mn	0.002	0.003	0.003
Ca	0.002	0.002	0.001
Ni	0.000	0.000	0.000
Sum	1.000	1.000	1.000
$F(X_i)$ (1)	0.266	0.697	0.364
k_D (4)	1.116	1.133	1.215
Mg# (2)	0.917	0.917	0.916
Fo	92.5	92.6	91.3

SP	CRSP1	CRSP4	CRSP3
MgO	17.7(3)	16.9(1)	17.0(2)
Al_2O_3	33.9(5)	33.8(3)	32.8(3)
FeO*	12.7(2)	12.6(2)	12.6(2)
Cr_2O_3	34.8(9)	34.9(4)	35.2(4)
NiO	0.22(4)	0.20(4)	0.17(5)
MnO	0.17(6)	0.17(4)	0.17(6)
TiO_2	0.25(2)	0.24(4)	0.24(4)
SiO_2	0.07(2)	0.05(2)	0.04(2)
ZnO	0.00	0.15(6)	0.00
Sum	99.81	99.01	98.22
T SITE			
Mg	0.659	0.653	0.652
Al	0.059	0.060	0.069
Fe^{2+}	0.244	0.245	0.245
Fe^{3+}	0.032	0.033	0.029
Mn	0.004	0.004	0.004
Si	0.002	0.002	0.001
Zn	0.000	0.003	0.000
Sum	1.000	1.000	1.000
M SITE			
Al	1.082	1.079	1.058
Cr	0.783	0.799	0.811
Mg	0.097	0.083	0.089
Fe^{2+}	0.001	0.015	0.015
Fe^{3+}	0.027	0.014	0.018
Ni	0.005	0.005	0.004
Ti	0.005	0.005	0.005
V	0.000	0.000	0.000
Sum	2.000	2.000	2.000
$F(X_i)$ (1)	0.102	0.070	0.036
k_D (5)	0.008	0.007	0.009
T (°C)	753.6	768.5	824.6

(1) $$F(X_i) = \frac{1}{n}\sum_{1}^{n}{}_j \left[\frac{O_j - C_j(X_i)}{s_j}\right]^2$$

(2) $Mg\# = Mg/Mg+Fe^{2+}$

(3) $R^{3+} = {}^{VI}Al+Cr^{3+}+Fe^{3+}+Ti^{4+}$

(4) $k_D = (Fe^{2+}/Mg)_{M1}/(Fe^{2+}/Mg)_{M2}$

(5) $k_D = Mg_M * Al_T / Mg_T * Al_M$

u is 0.2628, as a mean. This positional parameter, the only one which varies in the spinel structure, is influenced by cation distribution, which in turn depends on the cooling history of the host rock, and yields higher values for lower cooling rates. Parameter *u* of the studied crystals is similar to that of Hannouba spinel (*u* = 0.2628) but slightly higher

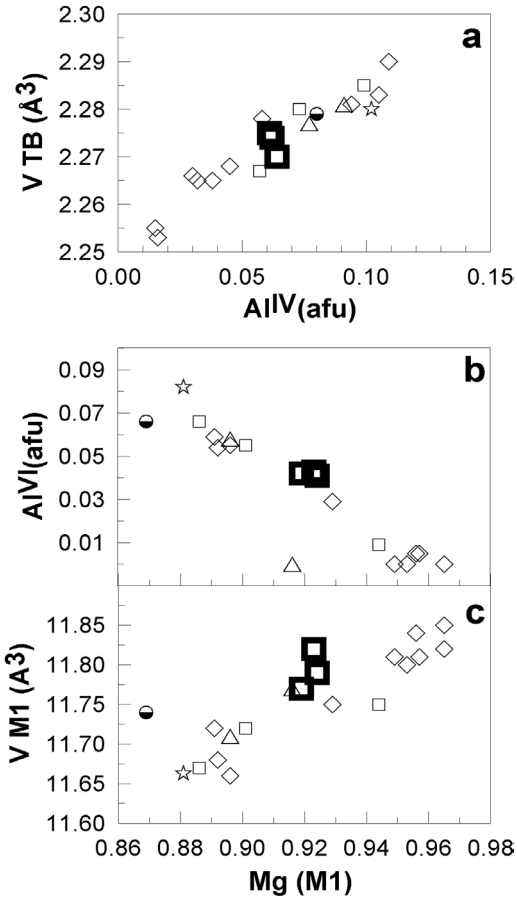

Fig. 3 – Al^{IV} *vs*. VTB (a), Mg (M1) content *vs*. Al^{VI} (b) and *vs*. VM1 (c) and for Predazzo opx;. Mantle xenolith opx from Mts. Leura, Noorat and Porndon, Australia (Cundari *et al*., 1986; Molin and Stimpfl, 1994), Cameroon (Princivalle *et al*., 1995) and Hannouba Region (China; Princivalle *et al*., 1998) are reported for comparison. Symbols as in Fig. 2.

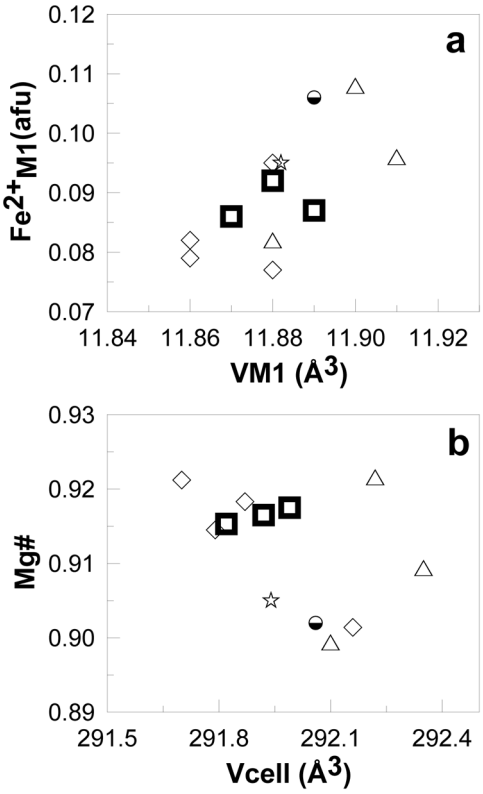

Fig. 4 – (a) VM1 *vs*. Fe^{2+} content in M1 site of Predazzo olivine; (b) V_{cell} *vs*. mg value. Mantle xenolith ol from Mts. Leura and Noorat., Australia (Cundari *et al*., 1986; Princivalle, 1990), Cameroon (Princivalle *et al*., 1995), and Hannouba Region (China; Princivalle *et al*., 1998) are reported for comparison. Symbols as in Fig. 2.

than those of spinels from the other compared samples (*u* = 0.2622-0.2626). Therefore, it is to be expected that the Predazzo and Hannouba crystals underwent a similar cooling history, slower than that of spinels from other compared localities.

Intra-crystalline relationships

The degree of Mg-Fe^{2+} intra-crystalline ordering in M1 and M2 sites of olivine, orthopyroxene and clinopyroxene is defined by the temperature at which the exchange between the two cations ceased. This cation distribution is represented by

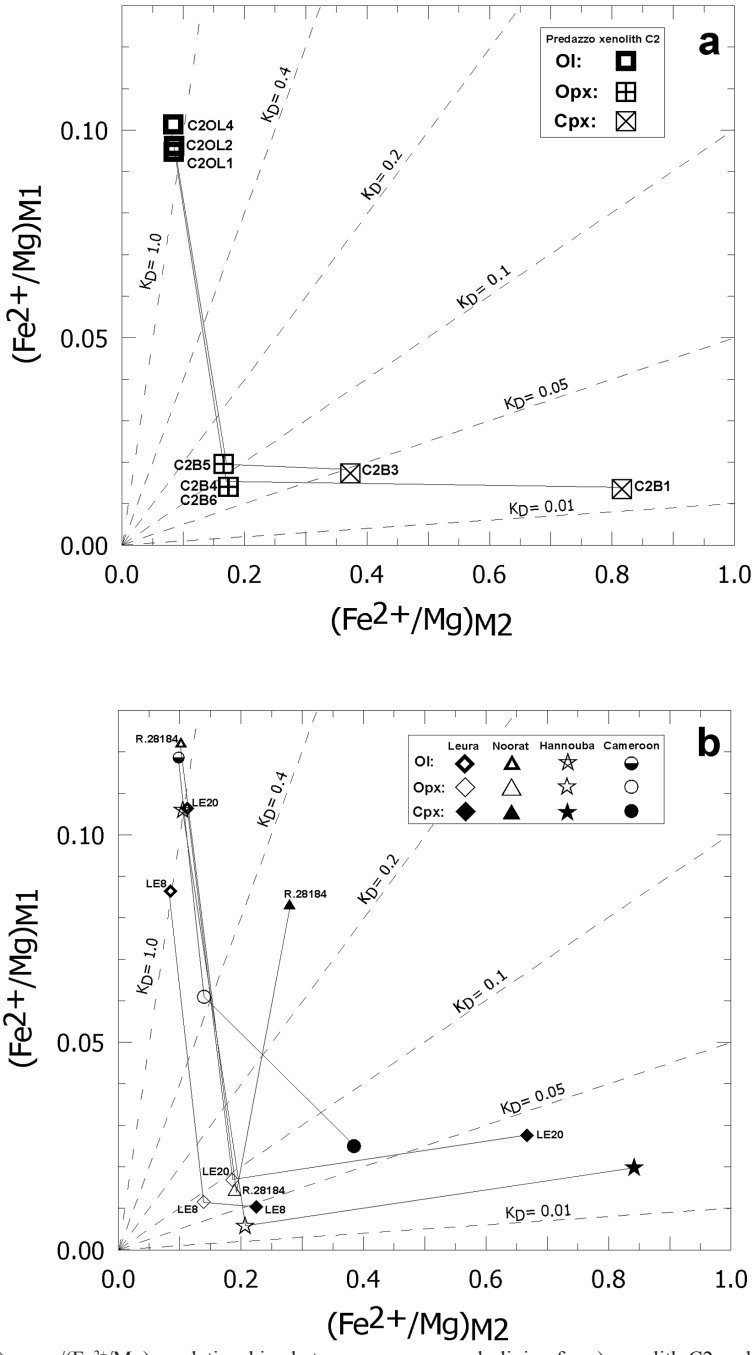

Fig. 5 – $(Fe^{2+}/Mg)_{M1}$ *vs.* $/(Fe^{2+}/Mg)_{M2}$ relationships between cpx, opx and olivine for a) xenolith C2 and b) representative samples analogue in composition from the literature. In both cases, tie-lines indicate coexisting silicatic phases. Note that opx from xenolith C2 are perfectly overlapped.

the equilibrium constant – $k_D = (Fe^{2+}/Mg)_{M1}/(Fe^{2+}/Mg)_{M2}$ – for the exchange reaction:

$$Mg_{M1}+Fe^{2+}_{M2} \leftrightarrow \mathbf{Fe^{2+}_{M1}}+Mg_{M2} \quad (1)$$

Fig. 5a shows the $(Fe^{2+}/Mg)_{M1}$ *vs*. $/(Fe^{2+}/Mg)_{M2}$ relationships for cpx, opx and ol phases coexisting in xenolith C2. Selected samples from the literature are reported in Fig. 5b for comparison. In both figures, k_D isopleths for the range of interest are indicated.

The k_D variation of Predazzo cpx is essentially a function of $(Fe^{2+}/Mg)_{M2}$. Similar behaviour is also shown by most of the cpx from Mt. Leura reported in Cundari *et al*. (1986), all falling below the k_D = 0.05 isopleth (*e.g*., samples LE8 and LE20; Fig. 5b). Morevover, Hannouba cpx shows Mg-Fe^{2+} intra-crystalline ordering in M1 and M2 sites similar to that of cpx C2B1; on the other hand, analogues from Cameroon and Mt. Noorat (*e.g*., sample R.28184) have slightly and significantly higher k_D values, respectively, than C2 samples.

Predazzo opx have k_D close to 0.1, higher than k_D values for coexisting cpx (Fig. 5a). This trend is consistent with cpx-opx pairs from Mt. Leura, Cameroon and Hannouba but different from that shown by opx from Mt. Noorat, for which a fall in k_D is observed (Fig. 5b). It is also to be noted that the Predazzo opx quite overlap sample LE20, which was considered an ultimate Fe^{2+} carrier during partial melting of the Australian mantle portion of interest (Molin and Stimpfl, 1994).

Predazzo ol have k_D values ranging from 1.05 to 1.25, and remain virtually unchanged with the increase/decrease in both $(Fe^{2+}/Mg)_{M1, M2}$. Similar behaviour is shown by ol from worldwide mantle xenoliths, the k_D of which is close to 1 in most cases.

As regards spinel, the degree of intracrystalline ordering, depending on temperature, is related to Mg-Al distribution between M and T structural sites. This is represented by the equilibration distribution coefficient – $k_D = Mg_MAl_T/Mg_TAl_M$ – of the intracrystalline exchange reaction:

$$Mg_T+Al_M \leftrightarrow \mathbf{Mg_M}+Al_T \quad (2)$$

The spinel k_D value, which strongly depends on temperature variation, is mainly a function of the inversion degree of spinel, but this dependence is quite complex (Carraro, 2003). However, it may be observed that, for CRSP1, CRSP3 and CRSP4 samples, the k_D value is low, and corresponds to that of spinels with the highest values of the Cr/(Cr+Al+Fe^{3+}) ratio, therefore indicating the most refractory compositions within each compared series.

Bearing in mind that reactions (1) and (2) are thermally activated, intra-crystalline closure temperatures were calculated using intra-crystalline geothermometers for cpx (Dal Negro *et al*., 1982) and opx (Stimpfl *et al*., 1999), based on the use of k_D and the empirical equation proposed by Princivalle *et al*. (1999) for spinel. Temperatures are reported in Tab. 3.

Values obtained for cpx C2B1 and C2B3 (T = 509 and 669 °C, respectively) are different from those reported in Carraro and Salviulo (1998) for the same crystals (T = 577 and 367 °C, respectively). Temperatures obtained for opx C2B4, C2B5 and C2B6 crystals (T = 635 °C, 774 °C and 644 °C, respectively) are also different from those previously reported for the same samples (T = 727 °C, 692 °C and 687 °C, respectively). In this latter case a modified and more recent thermometric calibration was applied (Stimpfl *et al*., 1999). On the whole, new closure temperatures obtained for both cpx and opx are significantly affected by the different refinement strategy used in this work, which in turn improved the cation distribution and therefore the estimation of T with appropriate intracrystalline geothermometers.

The mean temperature value for cpx (589±80 °C) is similar to T-value reported for Hannouba cpx (558±50 °C) but lower than those for Mt. Leura cpx (about 700 °C). The mean temperature value for opx (684±64 °C) is higher than that of the Hannouba opx (408±50 °C).

The mean intracrystalline temperature value obtained for spinel crystals CRSP1, CRSP3 and CRSP4 (T_{mean} = 782±31 °C) is slightly higher than reported for Hannouba spinel (710±50 °C) and lower than those for the Mt. Leura spinels (about 850 °C).

Equilibration pressure

Equilibration pressure for mineral pairs of cpx-ol grains from thin sections of some Predazzo mantle xenoliths were estimated using the Ca-in-ol geobarometer of Köhler and Brey (1990),

giving reliable values from 1.2 to 1.6 GPa (Carraro and Visonà, 2003), consistent with the stability conditions of the spinel peridotite field. In this paper, we attempted to obtain equilibration pressure values from single crystals C2OL1, C2OL2 and C2OL4, in order totally to avoid the possible effects of secondary fluorescence, due to the presence of the cpx phase at the boundary of olivine – the so-called Phase Boundary Fluorescence effect (PBF) – (Köhler and Brey, 1990). Ca profiles of the studied samples are shown in Fig. 6, in which the interval of the Ca content on the y axis is particularly reduced, in order to emphasise Ca variations within single crystals. Olivine crystals show elevated Ca contents in the outermost 30-40 micron, as also observed in Carraro and Visonà (2003) for greater non-isolated grains. In this case, higher Ca amounts in the rims (and consequently lower equilibration pressures) cannot be the result of the PBF effect because analyses were made on very small isolated grains, each mounted on glass slides.

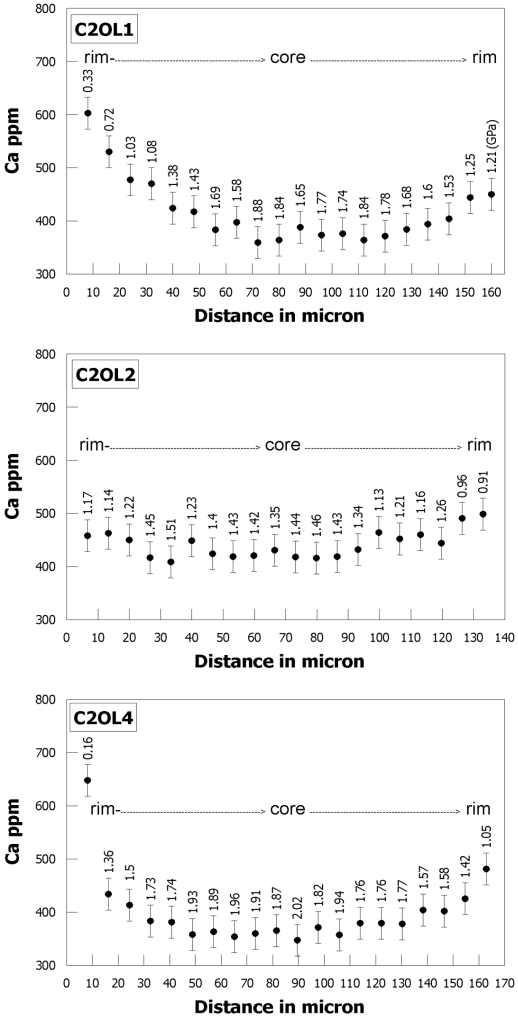

Fig. 6 – Ca zoning profile rim-core-rim for olivine single crystals from Predazzo. Values of equilibration pressure calculated with Ca-in-ol geobarometer are reported for each measured Ca content.

Mean pressure values obtained for the central zones of olivine crystals, with almost constant Ca contents, are 1.75±0.1, 1.37±0.1 and 1.86±0.1 GPa for samples C2OL1, C2OL2 and C2OL4, respectively, suggesting a mean equilibration pressure of about 1.5 GPa, close to the values reported by Carraro and Visonà (2003).

Discussion and conclusions

The constituent phases of the spinel lherzolite xenolith from Predazzo show crystal chemical behaviour similar to that of world-wide clinopyroxene, orthopyroxene, olivine and spinel, which formed upper mantle xenoliths with protogranular texture. The cation distributions of the four phases therefore reflect thermal events, which involved a mantle portion under the Dolomites and from which the observed mineral assemblage and protogranular texture resulted. In particular, correlation between the modal composition and crystal chemistry of cpx is consistent with the hypothesis that this mantle xenolith is one of the fragments of the most refractory mantle portion resulting from partial upper mantle melting under the Dolomite region. This is also supported by the fact that the coexisting spinel has high values of the $Cr/(Cr+Al+Fe^{3+})$ ratio, which correspond to the most refractory compositions within the previously studied serie of Predazzo Cr-spinels (Carraro, 2003). Moreover, according to the equation proposed by Hellebrand *et al.* (2001), the degree of fractional melting for the mantle lherzolite portion considered in this study, as a function of Cr#, falls in the range 14.81-15.10, corresponding to the most depleted compositions.

Treatment of cpx and opx X-ray data with the SHELXL-93 structure refinement program provides better results with respect to those obtained from the STRUCSY program for the same crystals (Carraro and Salviulo, 1998). Note that, performing refinements against Fo^2, using all data - rather than only data with *Fo* greater than a specified threshold - and considering also weak reflections, a real improvement in the structure refinement results was obtained: R1 was lower than 3% and $F(X_i)$ values (Tab. 3), related to cation distribution, were lower than 1 in all cases. This fact means that cation distributions and k_D values are high-quality data, capable of yielding more reliable closure temperature values.

Although the limitations due to the high complexity of the compositions of interest, the intra-crystalline temperature values estimated for cpx, opx and spinel with different appropriate calibrations can be considered realistic: in all cases, they indicate that the cooling rate of the host rock was relatively fast, but slower than that typical of volcanic rocks (*e.g.*, Australian samples). This is consistent with the subvolcanic conditions in which the Triassic mafic alkaline dyke (camptonite) cooled.

Ca zoning profiles observed in olivine single crystals are not a consequence of secondary fluorescence. The same behaviour is also indicated by many peridotitic olivine single grains reported in the literature (Köhler and Brey, 1990). This means that the increase in Ca at the rims of the studied olivine crystals is exclusively due to high diffusion of Ca in this phase and is therefore the result of decompression and/or heating by the host magma, thus confirming the hypothesis suggested by Carraro and Visonà (2003).

Acknowledgements

The author is very grateful to Profs. Antonio Della Giusta and Francesco Princivalle for constructive discussion and useful suggestions. Profs. Dario Visonà and Susanna Carbonin are thanked for their encouragement in writing this paper. An anonymous referee also greatly improved the manuscript.

Microprobe analyses were performed at the C.N.R. – Istituto di Geoscienze e Georisorse (Padova) – and C.N.R.S. (Camparis Centre, Paris VI). The assistance and cooperation of R. Carampin (Padova), H. Remy and M. Fialin (Paris VI) during collection data are gratefully acknowledged. G. Walton revised the English text. The author also gratefully acknowledges financial support from the University of Padova.

REFERENCES

Carraro A. (2003) – *Crystal chemistry of Cr-spinels from a suite of spinel peridotite mantle xenoliths from the Predazzo Area (Dolomites, Northern Italy)*. Eur. J. Mineral., **15**, 681-688.

Carraro A. and Salviulo G. (1998) – *Pressure and temperature estimates from crystal chemical studies of pyroxenes in spinel lherzolite xenoliths from the Predazzo Igneous Complex, Dolomites Region, North Italy*. N. Jb. Miner. Mh., **12**, 529-544.

Carraro A. and Visonà D. (2003) – *Mantle xenoliths in Triassic camptonite dykes of the Predazzo Area (Dolomites, Northern Italy): petrography, mineral chemistry and geothermobarometry*. Eur. J. Mineral., **15**, 103-115.

Cundari A., Dal Negro A., Piccirillo E.M., Della Giusta A. and Secco L. (1986) – *Intracrystalline relationships in olivine, orthopyroxene, clinopyroxene and spinel from Mt. Noorat, Victoria, Australia*. Contrib. Mineral. Petrol., **94**, 523-532.

Dal Negro A., Carbonin S., Molin G.M., Cundari A. and Piccirillo E.M. (1982) – *Intracrystalline cation distribution in natural clinopyroxenes of tholeiitic, transitional and alkaline basaltic rocks*. In "*Advances in physical geochemistry*", S.K. Saxena, ed. Springer Verlag, Berlin, Heidelberg, New York, **2**, 117-150.

Dal Negro A., Carbonin S., Domeneghetti C., Molin G.M., Cundari A. and Piccirillo E.M. (1984) – *Crystal chemistry and evolution of the clinopyroxene in a suite of high pressure ultramafic nodules from the Newer Volcanics of Victoria, Australia*. Contrib. Mineral. Petrol., **86**, 221-229.

Della Giusta A., Ottonello G. and Secco L. (1990) – *Precision estimates of interatomic distances using site occupancies, ionization potentials and polarizability in Pbnm silicate olivines*. Acta Crystallogr., **46**, 160-165.

Domeneghetti M.C., Molin G.M., Triscari M. and Zema M. (2000) – *Orthopyroxene as a geospeedometer: Thermal history of Kapoeta, Old Homestead 001, and Hughes 002 howardites*. Meteorit. Planet. Sci., **35**, 347-354.

Hellebrand E., Snow J.E., Dick H.J.B. and Hofman

A.W. (2001) – *Coupled major and trace elements as indicators of the extent of melting in mid-ocean-ridge peridotites*. Nature, **410**, 677-681.

International Tables for X-ray Crystallography (1974): Kynoch Press, Birmingham GB, **4**, 99-101.

Köhler T.P. and Brey G.P (1990) – *Calcium exchange between olivine and clinopyroxene calibrated as a geothermobarometer for natural peridotites from 2 to 60 kb with applications*. Geochim. Cosmochim. Acta, **54**, 2375-2388.

Lavina B., Salviulo G. and Della Giusta A. (2002) – *Cation distribution and structure modelling of spinel solid solutions*. Phys. Chem. Minerals, **29**, 10-18.

Molin GM. and Stimpfl M. (1994) – *Crystal chemistry and intracrystalline relationships of orthopyroxene in a suite of high pressure ultramafic nodules from the "Newer Volcanics" of Victoria, Australia*. Mineral. Mag., **58**, 325-332.

Morimoto N. (1988) − *Nomenclature of pyroxenes*. Mineral. Mag., **52,** 535-550.

Princivalle F., Della Giusta A. and Carbonin S. (1989a) – *Comparative crystal chemistry of spinels from some suites of ultramafic rocks*. Mineral. Petrol., **40**, 117-126.

Princivalle F., Salviulo G., Fabro C. and Demarchi G. (1994) – *Inter- and intra-crystalline temperature and pressure estimates on pyroxenes from NE Brazil mantle xenoliths*. Contrib. Mineral. Petrol., **116**, 1-6.

Princivalle F., Salviulo G., Marzoli A., Tirone M. and Nyobe J.B. (1995) – *Crystal chemistry of the constituent phases of a spinel peridotite nodule from Cameroon Volcanic Line (W-Africa)*. Miner. Petrogr. Acta, **38**, 1-8.

Princivalle F., Salviulo G. and Demarchi G. (1999) – *Crystal chemistry of clinopyroxenes in spinel-peridotite mantle xenoliths from the Fernando de Noronha oceanic island (NE Brazil)*. Miner. Petrogr. Acta, **42**, 103-112.

Princivalle F., Salviulo G., Marzoli A. and Piccirillo E.M. (2000a) – *Clinopyroxene of spinel-peridotite mantle xenoliths from Lake Nji (Cameroon Volcanic Line, W Africa): crystal chemistry and petrological implications*. Contrib. Mineral. Petrol., **139**, 503-508.

Princivalle F. and Secco L. (1985) – *Crystal structure refinement of 13 olivines in the Forsterite-Fayalite series from volcanic rocks and ultramafic nodules.* Tschermaks Min. Petr. Mitt., **34**, 105-115.

Princivalle F., Secco L. and Demarchi G. (1989b) – *Crystal chemistry of a clinopyroxene series in ultramafic xenoliths from North-Eastern Brazil*. Contrib. Mineral. Petrol., **101**, 131-135.

Princivalle F., Tirone M. and Comin-Chiaramonti P. (2000b) – *Clinopyroxenes from metasomatized spinel-peridotite mantle xenoliths from Nemby (Paraguay): crystal chemistry and petrological implications*. Mineral. Petrol., **70**, 25-35.

Princivalle F., Wanming Y., Feng J. and Comin-Chiaramonti P. (1998) – *Crystal chemistry of the constituent phases of a spinel peridotite xenolith from Hannouba Region (China)*. Miner. Petrogr. Acta, **41**, 35-42.

Rossi G., Oberti R., Dal Negro A., Molin G.M. and Mellini M. (1987) – *Residual electron density at the M2 site in C2/c clinopyroxenes: relationships with bulk chemistry and sub-solidus evolution*. Phys. Chem. Mineral., **14**, 514-520.

Sheldrick G.M. (1993) – *SHELXL-93. Program for crystal structure refinement*. University of Göttingen, Germany.

Stimpfl M., Ganguly J. and Molin G.M. (1999) – *Fe^{2+}-Mg order-disorder in orthopyroxene: equilibrium fractionation between the octahedral sites and thermodynamic analysis*. Contrib. Mineral. Petrol., **136**, 297-309.

Tokonami M. (1965) – *Atomic scattering factor for O^{2-}*. Acta Crystallogr., **19**, 486.